Review Article

Ultra-small superparamagnetic iron oxide contrast agents for lymph node staging of high-risk prostate cancer

Marcin Czarniecki[1], Filippo Pesapane[2,3], Bradford J. Wood[3], Peter L. Choyke[1], Baris Turkbey[1]

[1]Molecular Imaging Program, National Cancer Institute, National Institutes of Health, Bethesda, MD, USA; [2]Postgraduate School in Radiodiagnostics, Università degli Studi di Milano, Milan, Italy; [3]Center for Interventional Oncology, NCI and Radiology Imaging Sciences, Clinical Center, National Institutes of Health, Bethesda, MD, USA

Contributions: (I) Conception and design: M Czarniecki, F Pesapane, B Turkbey; (II) Administrative support: None; (III) Provision of study material or patients: None; (IV) Collection and assembly of data: None; (V) Data analysis and interpretation: None; (VI) Manuscript writing: All authors; (VII) Final approval of manuscript: All authors.

Correspondence to: Baris Turkbey, MD. Molecular Imaging Program, National Cancer Institute, 10 Center Dr, MSC 1182, Building 10, Room B3B85, Bethesda, MD 20892-1088, USA. Email: turkbeyi@mail.nih.gov.

Abstract: Ultrasmall superparamagnetic particles of iron oxide (USPIOs) imaged with magnetic resonance imaging (MRI) have been proposed as an experimental method for visualizing lymph node (LN) metastases. The method does not require ionizing radiation, yet can detect small nodes that are involved with metastases. USPIOs are naturally taken up by macrophages that deposit in the normal LN creating a low signal region in normal areas; areas within the node that do not show this loss of signal are likely involved by tumor although there can be other causes (fibrosis or inflammation). However, the lack of approved USPIOs that are clinically available hinders adoption and larger studies. The proposed indications for USPIO MRI, including specific compounds and imaging methods are discussed.

Keywords: Ultrasmall superparamagnetic particles of iron oxide (USPIO); lymph node (LN); prostate cancer; magnetic resonance imaging (MRI)

Submitted Mar 15, 2018. Accepted for publication May 15, 2018.
doi: 10.21037/tau.2018.05.15
View this article at: http://dx.doi.org/10.21037/tau.2018.05.15

Introduction

Detection of lymph node (LN) metastasis is an important prognostic marker and has a strong impact on prostate cancer (PCa) management. Currently, the decision to perform pelvic lymph node dissection (PLND) as part of a radical prostatectomy is based on available local staging with imaging and clinical nomograms. To assess nodal staging, MRI and CT are most commonly used, however, these conventional techniques have poor sensitivity (1). Both MRI and CT perform equally poorly for assessing LNs as both are based on morphology and size features which are notoriously insensitive to small tumor deposits which do not significantly alter the size or shape of LNs. Since direct methods of imaging LN metastases are limited, several nomograms have been developed that calculate LN metastatic risk based on clinical parameters and T staging that correlates to some degree with N staging. However, these methods cannot localize the sites of LN metastases but merely forecast the likelihood that one or more malignant nodes may be present in the case (2-4). More recently, functional and molecular imaging methods have been proposed as alternatives (1).

Current radiological interpretation of LNs is based on the presence of a fatty hilum, a small (typically <0.8–1.0 cm) short axis diameter, a relatively higher signal intensity (SI) than normal on T2-weighted images (T2WI), and a regular capsular appearance, all of which indicate a normal LN (5). Micrometastases, that do not alter LN size or morphology often leads to false-negative results. In contrast, tumor-infiltrated nodes are classically considered to be larger, have replaced fatty hila and may appear irregular. However, these

findings are subjective.

A recent meta-analysis of MRI in LN metastases detection showed a pooled sensitivity and specificity per patient of 56% (95% CI, 0.42–0.69) and 94% (95% CI, 0.90–0.96), respectively (6). In this study, normal-sized LNs showed a slightly higher sensitivity (59%, 95% CI, 0.26–0.93) than all the pooled studies irrespective of LN size (0.56, 95% CI, 0.42–0.69). It was speculated that most of the studies that were included in the meta-analysis which were shown to be tumor positive with normal LN size were using ultrasmall superparamagnetic particles of iron oxides (USPIOs) indicating their possible use in the setting of small LN metastases. These results suggest that current imaging methods are not adequate for the detection of metastatic LNs, but further technical issues must still be addressed (7). General principles in USPIO imaging, approved compounds, and other available imaging methods are discussed in this review.

Methods

A systematic review was performed on PubMed in peer-reviewed journals published from 1990 to 2018 in English using the terms: USPIO, ferumoxytol, ferumoxtran, MR lymphangiography, and ultra-small paramagnetic iron oxide. The following criteria were included: (I) studies with patients undergoing ferumoxtran-10 imaging, (II) studies with patients undergoing ferumoxytol imaging, (III) physical properties of ultra-small paramagnetic iron oxide particles. Additionally, information on the Food and Drug Administration (FDA) website was used as well as singular sources to give the context of use of USPIOs.

General principles of USPIO in MRI

The rationale for the use of USPIO is that, after intravenous injection, the nanoparticles are phagocytosed by macrophages in circulation which then enter the interstitial space and are taken up by lymphatics into LNs (8-11). Once within the LN, iron-laden macrophages remain for several days before the iron begins to be processed into iron stores. Since iron oxide is superparamagnetic, it becomes strongly magnetic in the strong magnetic field of the MRI leading to spin dephasing and susceptibility effects, which result in signal loss. Therefore, the SI is markedly reduced in normal LN tissue due to the magnetic susceptibility and T2 shortening effects of the USPIO particles (8,12). Conversely, in areas of LNs replaced by malignant cells there is much less uptake of USPIO particles and, therefore, those portions of the LNs remain unchanged in signal on T2WI and T2*-weighted imaging (T2*WI) 24–48 hours after intravenous injection of a USPIO (8-11).

Several studies (9,10,12-14) hypothesized that the lack of USPIO uptake (partial or total) in metastatic LNs is because normal iron-laden macrophages cannot enter into collections of tumor cells within the LN (15). Although two different studies (16,17) histologically correlated USPIO-uptake with normal macrophage activity, no study has yet localized USPIO particles to specific intra-cellular components in healthy LNs (15). Since benign LNs usually contain mostly T-cells and only few macrophages, the question is whether USPIO particles are transferred to other cell types in the LN (15). Moreover, some tumoral uptake of USPIO particles in intracranial tumors has been demonstrated (18-20). Daldrup-Link *et al.* (15) suggested that other immune cell types, such as dendritic cells, may play a role in the USPIO-retention in LNs.

The MRI performed after administration of USPIOs provides more information than conventional anatomic imaging by showing normal homogeneous uptake (loss of signal) in healthy LNs. The presence of USPIOs within the LN shortens the T2WI and T2*WI relaxation time decreasing the SI on MRI (*Figure 1*). Metastatic LNs take up the USPIO either partially or not at all, with tumor retaining the same SI or having a slightly higher SI compared to the SI prior to USPIO administration (*Figure 2*) (8). T2*WI effects of iron oxides resulting in loss of SI are due to static dephasing of spins. T2WI is also affected but to a lesser degree due to rephasing gradients (21).

Criteria for determining whether a LN is metastatic on USPIO MRI have been developed (7-10,12-14,22). The following criteria are used when interpreting T2-weighted USPIO-enhanced MRI: (I) complete involvement; no signal loss or hyperintensity after USPIO throughout the whole LN; (II) partial central involvement; high signal centrally with peripheral loss of SI along with heterogeneous architecture; (III) partial patchy involvement; signal loss whereby >50% of the node has areas of high SI with heterogeneous architecture. High SI in <50% of nodes with heterogeneous architecture should be considered as possibly metastatic (23). It should be noted that such definitions are not yet standardized or codified by an international organization.

To perform a USPIO-enhanced MRI, the following factors should be considered carefully: dosing, timing of imaging after USPIO injection, imaging parameters

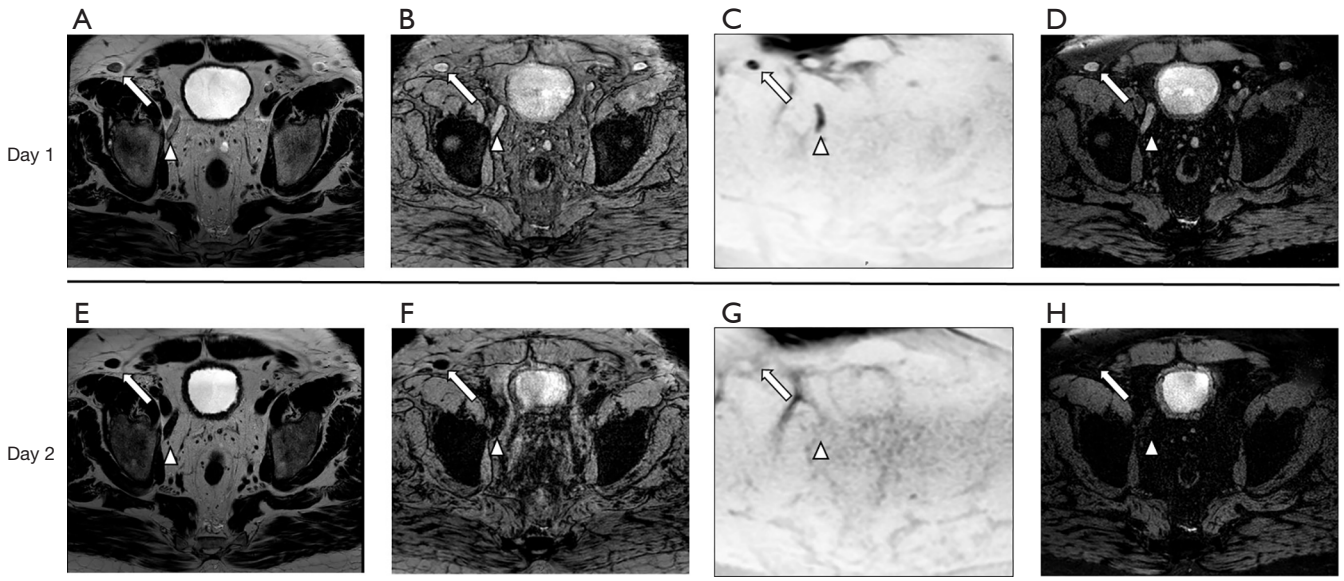

Figure 1 Ferumoxytol enhanced MR Lymphography findings of benign hyperplastic lymph nodes. (A-D) Pre-administration of ferumoxytol; (E-H) 24 hours post-administration images. (A,E) T2-weighted images; (B,F) T2* axial images; (C,G) diffusion-weighted images; (D,H) T2* spectral pre-saturation with inversion recovery (SPIR) images. A 57-year-old male with T3 high-grade papillary urothelial carcinoma. Two enlarged lymph nodes were seen, one in the right inguinal chain (arrow) and one in the right iliac chain (arrowhead). After administration of Ferumoxytol a signal diffuse signal loss is seen in these lymph nodes indicating benign hyperplasia, later seen on biopsy.

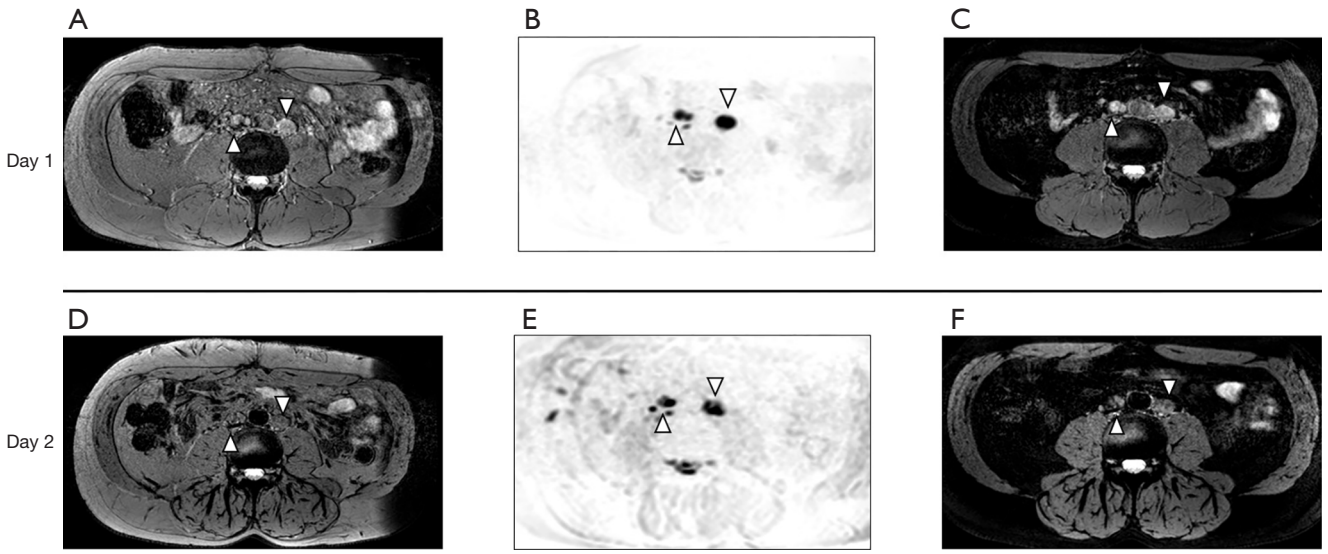

Figure 2 Ferumoxytol enhanced MR Lymphography findings of metastatic lymph nodes. (A-C) Pre-administration of ferumoxytol; (D-F) 24 hours post-administration images. (A,D) T2* axial images; (B,E) diffusion-weighted images; (C,F) T2* spectral pre-saturation with inversion recovery (SPIR) images. A 43-year-old male with Gleason 5+5 cancer, previously treated with radical prostatectomy and external beam radiotherapy. Enlarged paraortic lymph nodes were seen (arrowheads). After administration of Ferumoxytol, these lymph nodes retain their signal indicating metastasis.

for T2*WI (the key sequence), section thickness and the imaging plane (8). Thin section axial images reduce partial volume artifacts, which allow for detection of smaller malignant LNs (8). In the pelvis, oblique coronal imaging planes may be needed to provide the location of the LNs in relation to the obturator nerve, which is of anatomic importance to the surgeon as LNs anterior to the obturator nerve are generally resected per routine but nodes posterior to the nerve are not typically removed unless there is unambiguous evidence of involvement (8).

Two separate MRI examinations are required for a USPIO MRI: before and after the administration of a USPIO, with the latter performed at least 24–36 h after the intravenous injection to allow for sufficient LN uptake (7,9,10,12,13,22-24). If the post-contrast MRI is performed prematurely, the lack of sufficient USPIO particle uptake within non-metastatic LNs may lead to erroneous characterization as malignant nodes (8,12). Harisinghani *et al.* in 2006 (23) suggested that it might be possible to obtain only one MRI after USPIO administration if the reader is highly experienced. However, some metastatic LNs are hypointense on T2WI and T2*WI at baseline (25), making this method prone to error (7).

Ferumoxtran-10

Ferumoxtran-10 (Combidex®, SPL Medical B.V., Nijmegen, The Netherlands) also known as Sinerem®, is a USPIO that is coated with a low-molecular-weight dextran, which is biodegradable (26,27). It has a serum half-life that ranges from 24–36 h (10,11), as established by early animal and human studies (28,29).

In the past 15 years, Ferumoxtran-10 has gained interest primarily in Europe and is currently under clinical development there (7,9,10,12,13,22-24) to improve LN imaging in pelvic cancers (bladder and PCa). It is not available in the United States and has only limited availability in the Netherlands.

Ferumoxtran-10 tissue enhancement of normal LN tissue can be maximized by increasing the applied magnetic field strength, by using high iron oxide doses (3–7 mg/kg) (30), by using gradient echo instead of spin echo sequences, and by using long echo times (15,21). This is important as it provides greater contrast between normal and abnormal LNs. However, increasing the sensitivity of the sequence for iron too much can result in "blooming artifact" that will eliminate signal from non-iron containing regions of the image, including LNs. The above-mentioned T2 shortening effects of Ferumoxtran-10 are due to the proton diffusion-dependent dephasing and signal decay and to the chemical exchange between iron-bound and free water protons (15,31). T2*WI effects of USPIO are due to static dephasing and exceed T2 effects (21), therefore T2*WI is the most sensitive sequence in Ferumoxtran-10-enhanced MRI (21).

In 2003, Harisinghani *et al.* (12) first published a large prospective study of LN imaging with Ferumoxtran-10–enhanced MRI in 80 patients undergoing prostatectomy and PLND for prostate cancer. In this study, 334 LNs were resected or biopsied for validation, and LN metastases were found in 63 LNs (19% of resected nodes) from 33 patients (41%). All patients with surgical nodal metastases were identified by Ferumoxtran-10 MRI and a node-by-node analysis showed a significantly higher sensitivity for Ferumxtran-10 MRI than for conventional MR imaging (90.5% versus 35.4%; $P \leq 0.001$).

In 2008, a large study with Ferumoxtran-10 MRI in 375 PCa patients (24) showed a sensitivity of 82% and a specificity of 93% for the detection of histologically-proven metastatic LNs at a magnetic field strength of 1.5 T. Better results were shown at field strengths of 3.0 T MRI in a study comparing image quality of Ferumoxtran-10—enhanced MRI at 1.5 and 3.0 T (32).

Three studies of Ferumoxtran-10 MRI combining prostate and bladder cancer using a field strength of 3.0 T were published from 2009 to 2013 by a Swiss research group (9,13,14). Birkhäuser *et al.* (9) prospectively assessed the diagnostic accuracy of Ferumoxtran-10 using conventional MRI sequences combined with diffusion-weighted imaging (USPIO-DW-MRI) in staging of normal-sized pelvic LNs in bladder and/or PCa patients. Seventy-five patients with clinically localized bladder and/or prostate cancer, staged previously as N0 by conventional cross-sectional imaging, were entered in this study. Combined USPIO-DW-MRI findings were analyzed by 3 independent readers and correlated with histopathologic LN findings after PLND and resection of primary tumors. Per-patient sensitivity and specificity for detection of metastatic LNs by the 3 readers were 65–75% and 93–96%, respectively. Note that enlarged LNs were eliminated from consideration in this study.

These results are consistent with the preliminary data obtained by Thoeny *et al.* (7) in their analogous study based on 21 patients. Both studies (7,9) showed the capability of USPIO-DW-MRI to detect metastases in normal-sized LNs (10). It was demonstrated by Meijer *et al.* that patients with positive LN by Ferumoxtran-10 that were ≤8 versus

>8 mm LN have a significantly better 5-year metastasis-free survival (79% versus 16%) and overall survival (81% versus 36%) (33).

Triantafyllou *et al.* (13) investigated 75 patients with bladder and/or prostate tumors with Ferumoxtran-10–enhanced MRI. A preoperative reading with 2 readers in consensus and a second postoperative reading with 3 independent blinded readers were performed and the results were correlated with histopathology. A total of 2,993 LNs were resected and examined histologically. Fifty-four metastatic LNs were found in 20 patients (26.7%). The average sensitivity of Ferumoxtran-10-enhanced MRI was 50%, with a specificity of 88.4% and a diagnostic accuracy of 81.8%. Poor reproducibility was observed among the three blinded readers regarding the presence or absence of metastatic disease in LNs (13).

The sensitivity values reported in several of the above-mentioned studies for Ferumoxtran-10 ranged from 50–75% (9,13,14) when considering only LNs that were normal in size. Although the specificity is quite good, generally >88% in most studies, the low sensitivity may limit the clinical utility. There are several factors that influence the sensitivity in such studies. In several studies, meticulous histopathology (34) was performed. This increases the number of microscopic LN metastases that are beyond the resolution of MRI. Another factor is the mixing of bladder and prostate cancer, which have different biological behaviors (35). If the mix favors bladder cancer, sensitivity is higher since this is an aggressive disease with fast growing LN metastases whereas if the mix favors prostate cancer, the nodes will be smaller and harder to detect. Finally, if T2WI is used rather than T2*WI (10,35) sensitivity will decrease. Several of these studies also employed diffusion-weighted imaging. Malignant nodes will tend to be high in signal whereas, benign nodes will tend to disappear after Ferumoxtran-10 is administered (7). This approach allows a substantial reduction of the interpretation time, as it simplified the reading of Ferumoxtran-10–enhanced MRI (34,35). Additionally, several studies showed metastatic LNs outside the standard PLND area and standard radiation field in a considerable number of patients (53–79%), suggesting a potential role of Ferumoxtran-10–enhanced MRI to avoid the underestimation of metastatic disease (9,13,14,33,36,37).

In 2011, Wu *et al.* (38) compared the diagnostic accuracy of USPIO-enhanced MRI with baseline MRI in various body regions for the detection of metastatic LNs in a meta-analysis consisting of 34 studies. USPIO-enhanced MRI showed an overall sensitivity of 95% and overall specificity of 95% versus an overall sensitivity of 39% and specificity of 90% on the baseline MRI. This meta-analysis showed that USPIO-enhanced MRI offers higher diagnostic performance than conventional MRI. Thus, there are small but important advantages to Ferumoxtran-10 enhanced LN imaging.

Pelvic nodal staging (N-staging) with Ferumoxtran-10–enhanced MRI presents several significant challenges. The first one is the availability of the agent, since in 2009 Combidex® was withdrawn from the registration process in Europe by the manufacturer (10). Since 2013, Ferumoxtran-10 is only available in the Netherlands (Europe), where it is made privately by the Radboud University Medical Center (Radboudumc) that obtained all licenses and documentation for the production process (10), and thus, there is currently limited access to it worldwide (7). Secondly, USPIO enhanced MRI is logistically inconvenient, requiring both a baseline MRI and a MRI after injection. Moreover, even though the Ferumoxtran-10–enhanced MRI can only be performed once (without the baseline MRI), as Harisinghani *et al.* suggested (23), the patient still needs to come to the hospital twice because USPIO has to be administered at least 24 hours prior to perform the MRI (7). Thirdly, the interpretation of LNs on the Ferumoxtran-10–enhanced MRI is highly subjective (13) and laborious because every LN must be compared on both sequences (7). Moreover, metastatic LNs ≤5 mm in diameter can be missed because of spatial resolution limits (7). Moreover, enlarged but healthy LNs can fail to take up the Ferumoxtran-10 USPIO because of severe inflammation or fibrosis, leading to false-positive results (7). Finally, due to concerns about iron overload, the study cannot be repeated too frequently.

A small number of adverse events have been reported with Ferumoxtran-10. These mainly relate to local side effects at the infusion site and serious and life-threatening anaphylactic reactions (10,15,39,40). The aggregate rate of anaphylaxis related to the use of USPIO was 0.02–0.2% (15,41). As rapid injection of USPIO particles can cause a distinct reaction (42), Ferumoxtran-10 must be administered slowly through a filtered needle to minimize infusion reactions, including other side effects such as low back pain, flushing, and nausea (39). The extravasation of USPIO particles can cause long-lasting skin discolorations that usually slowly disappear over time (15,43). Commonly, Ferumoxtran-10 does not cause local inflammatory reactions. However, rarely, extravasated USPIO particles

have caused granulomas, dermatitis, or local fibrosis (15).

In 2009, Bernd *et al.* (39) reported safety data of 37 clinical trials with a total of 1,663 patients who underwent Ferumoxtran-10–enhanced MRI. Adverse events were reported in 23% of patients subdivided into Grade 1 mild (55%), Grade 2 moderate (30%), Grade 4 severe (12%), and Grade 5 serious (3%). Recently, Fortuin *et al.* (10) reported adverse events in 310 patients with PCa and an intermediate to high risk for metastatic LNs who underwent Ferumoxtran-10–enhanced MRI between January 2014 and July 2016. Eight of 310 patients (2.6%) had significant adverse effects including minor low back pain, flushing, nausea and dry mouth that disappeared in all before they left the hospital. The absence of moderate or serious (Grades 2–5) Ferumoxtran-10-related adverse events in this study (10) may be explained by the implementation of the following precautions: dilution of USPIO particles, very slow injection rate, and immediate discontinuation of the infusion upon complaints. They also used a filter in the infusion line to prevent injection of iron oxide aggregates, although this practice has recently been questioned (15).

Ferumoxytol

Ferumoxytol (Feraheme, AMAG Pharmaceuticals, Cambridge, MA, USA) is the only available iron oxide-containing compound for parenteral use in the United States. The FDA has approved the use of ferumoxytol for the treatment of iron deficiency anemia in adult patients with chronic kidney disease (CKD). All other medical uses including imaging are considered off-label. The compound has been investigated in LN imaging, but it has been studied less extensively than Ferumoxtran-10. Recent pilot studies have investigated optimal dosage, which is known to be higher than for ferumoxytran-10 and above the upper limit advised by the FDA for treatment of anemia (44). Approximately 2-fold more ferumoxytol must be administered to get comparable imaging results to Ferumoxtran-10. This likely relates to the surface coating of ferumoxytol with less uptake by macrophages.

Like ferumoxtran-10, the imaging protocol with ferumoxytol usually consists of a 2-day study with imaging prior to administration and 24 hours thereafter, which is the time-point that has been shown to elicit the highest concentration of the compound in LNs (45,46). The initial study by Harisinghani *et al.* attempted to use a similar dosing of ferumoxytol as was used with ferumoxtran-10 (4 mg Fe per kg). Although clinically usable results were obtained in this study, the ferumoxytol study was much more difficult to interpret and showed less tumor to background contrast than Ferumoxtran-10. Further studies had to establish optimal dosing, and a recent phase I study performed by Turkbey *et al.* aimed to establish the optimal dose that would result in a uniform signal loss of benign LNs like the appearance of previous Ferumoxtran-10 imaging results. This study demonstrated that the highest mean percentage change in SI was established with the highest dosage infused in the study (7.5 ng/mL) with a drop in SI by –65.1%. Future studies may use this experience to investigate more clinical applications for the compound. Like other USPIO particles, the FDA issued a number of statements on potential risks that are to be weighed prior to the administration of ferumoxytol (47). A diluted form of ferumoxytol is recommended to be administrated over a minimum of 15 minutes with saline, with all patients monitored throughout the infusion for changes in blood pressure and pulse for at least 30 minutes after the infusion has ended. This is due to the previously reported serious adverse events (SAE) of anaphylactic shock and cardiovascular collapse associated with this class of agent. The most commonly experienced adverse events include arthralgias, headache, and chest tightness, with no SAEs reported in a group of 60 patients (48). Although the risk of anaphylaxis is small, it nonetheless exists and the compounds administration is discouraged by the FDA in patients with multiple allergies, serious medical conditions, and the elderly (47).

Like ferumoxtran-10, ferumoxytol nanoparticles are retained in normal LNs due to macrophage phagocytosis, causing a T2* signal drop on T2*WI. Metastatic LNs, on the other hand, retain their original characteristics of relatively high signal in post-contrast images (15). Little is known about its performance in metastatic LN detection, but the recent dose escalation study confirms optimal doses for future work. This dose is slightly higher than the recommended dose for iron replacement therapy. Therefore, ferumoxytol-enhanced LN imaging studies should be performed with approval by regulatory agencies. A comparison of the two available compounds, Ferumoxytol and Ferumoxtran-10 are needed to compare their efficacy. Due to current restrictions by regulatory bodies, these compounds are not simultaneously available in one location and this lowers the possibility of such comparative studies any time soon.

Other considerations

While developments in USPIO imaging for LN metastases

are interesting and potentially important, there have been developments in positron emission tomography (PET) agents for LN detection prostate cancer that warrant consideration. For prostate cancer, the newest PET agent is prostate specific membrane antigen (PSMA)-directed. PET agents based on ligands with high binding affinity for PSMA have shown remarkable sensitivity for LN metastases in high risk patients. Such studies are relatively straightforward to interpret and when combined with CT or MRI can provide approximately the same spatial resolution as USPIO enhanced MRI. These agents, however, are not yet available widely.

Conclusions

Pre-operative assessment of LN staging in PCa is crucial for proper treatment selection and planning the extent of surgery or radiation in high-risk disease. Currently, the guidelines of when to perform limited versus extended PLND are limited and inconclusive. The use of anatomic imaging is limited both in sensitivity and specificity.

New imaging modalities including USPIOs enhanced MRI have shown promising results but mainly in the clinical research setting. Such agents will require further investigation to determine their clinical utility. Meanwhile, developments in PET agents targeting PSMA promise to overtake MR LN imaging in sensitivity and specificity.

Acknowledgements

The research in this study was funded by the Intramural Research Program of the National Institutes of Health.

Footnote

Conflicts of Interest: The authors have no conflicts of interest to declare.

References

1. Hövels AM, Heesakkers RA, Adang EM, et al. The diagnostic accuracy of CT and MRI in the staging of pelvic lymph nodes in patients with prostate cancer: a meta-analysis. Clin Radiol 2008;63:387-95.
2. Park SY, Oh YT, Jung DC, et al. Prediction of Micrometastasis (< 1 cm) to Pelvic Lymph Nodes in Prostate Cancer: Role of Preoperative MRI. AJR Am J Roentgenol 2015;205:W328-34.
3. Soylu FN, Peng Y, Jiang Y, et al. Seminal vesicle invasion in prostate cancer: evaluation by using multiparametric endorectal MR imaging. Radiology 2013;267:797-806.
4. Barentsz JO, Richenberg J, Clements R, et al. ESUR prostate MR guidelines 2012. Eur Radiol 2012;22:746-57.
5. Thoeny HC, Froehlich JM, Triantafyllou M, et al. Metastases in normal-sized pelvic lymph nodes: detection with diffusion-weighted MR imaging. Radiology 2014;273:125-35.
6. Woo S, Suh CH, Kim SY, et al. The Diagnostic Performance of MRI for Detection of Lymph Node Metastasis in Bladder and Prostate Cancer: An Updated Systematic Review and Diagnostic Meta-Analysis. AJR Am J Roentgenol 2018;210:W95-W109.
7. Thoeny HC, Barbieri S, Froehlich JM, et al. Functional and Targeted Lymph Node Imaging in Prostate Cancer: Current Status and Future Challenges. Radiology 2017;285:728-43.
8. Harisinghani MG, Dixon WT, Saksena MA, et al. MR lymphangiography: imaging strategies to optimize the imaging of lymph nodes with ferumoxtran-10. Radiographics 2004;24:867-78.
9. Birkhäuser FD, Studer UE, Froehlich JM, et al. Combined ultrasmall superparamagnetic particles of iron oxide-enhanced and diffusion-weighted magnetic resonance imaging facilitates detection of metastases in normal-sized pelvic lymph nodes of patients with bladder and prostate cancer. Eur Urol 2013;64:953-60.
10. Fortuin AS, Brüggemann R, van der Linden J, et al. Ultra-small superparamagnetic iron oxides for metastatic lymph node detection: back on the block. Wiley Interdiscip Rev Nanomed Nanobiotechnol 2018;10.
11. Corot C, Robert P, Idée JM, et al. Recent advances in iron oxide nanocrystal technology for medical imaging. Adv Drug Deliv Rev 2006;58:1471-504.
12. Harisinghani MG, Barentsz J, Hahn PF, et al. Noninvasive detection of clinically occult lymph-node metastases in prostate cancer. N Engl J Med 2003;348:2491-9. Erratum in: N Engl J Med 2003;349:1010.
13. Triantafyllou M, Studer UE, Birkhäuser FD, et al. Ultrasmall superparamagnetic particles of iron oxide allow for the detection of metastases in normal sized pelvic lymph nodes of patients with bladder and/or prostate cancer. Eur J Cancer 2013;49:616-24.
14. Thoeny HC, Triantafyllou M, Birkhaeuser FD, et al. Combined ultrasmall superparamagnetic particles of iron oxide-enhanced and diffusion-weighted magnetic resonance imaging reliably detect pelvic lymph node

metastases in normal-sized nodes of bladder and prostate cancer patients. Eur Urol 2009;55:761-9.
15. Daldrup-Link HE. Ten Things You Might Not Know about Iron Oxide Nanoparticles. Radiology 2017;284:616-29.
16. Koh DM, Brown G, Temple L, et al. Rectal cancer: mesorectal lymph nodes at MR imaging with USPIO versus histopathologic findings--initial observations. Radiology 2004;231:91-9.
17. Xue HD, Lei J, Li Z, et al. Lymph node image with ultrasmall superparamagnetic iron oxide and comparison with pathological result. Zhongguo Yi Xue Ke Xue Yuan Xue Bao 2009;31:139-45.
18. Varallyay P, Nesbit G, Muldoon LL, et al. Comparison of two superparamagnetic viral-sized iron oxide particles ferumoxides and ferumoxtran-10 with a gadolinium chelate in imaging intracranial tumors. AJNR Am J Neuroradiol 2002;23:510-9.
19. Zimmer C, Weissleder R, Poss K, et al. MR imaging of phagocytosis in experimental gliomas. Radiology 1995;197:533-8.
20. Moore A, Marecos E, Bogdanov A Jr, et al. Tumoral distribution of long-circulating dextran-coated iron oxide nanoparticles in a rodent model. Radiology 2000;214:568-74.
21. Henning TD, Wendland MF, Golovko D, et al. Relaxation effects of ferucarbotran-labeled mesenchymal stem cells at 1.5T and 3T: discrimination of viable from lysed cells. Magn Reson Med 2009;62:325-32.
22. Anzai Y, Piccoli CW, Outwater EK, et al. Evaluation of neck and body metastases to nodes with ferumoxtran 10-enhanced MR imaging: phase III safety and efficacy study. Radiology 2003;228:777-88.
23. Harisinghani MG, Saksena MA, Hahn PF, et al. Ferumoxtran-10-enhanced MR lymphangiography: does contrast-enhanced imaging alone suffice for accurate lymph node characterization? AJR Am J Roentgenol 2006;186:144-8.
24. Heesakkers RA, Hövels AM, Jager GJ, et al. MRI with a lymph-node-specific contrast agent as an alternative to CT scan and lymph-node dissection in patients with prostate cancer: a prospective multicohort study. Lancet Oncol 2008;9:850-6.
25. Froehlich JM, Triantafyllou M, Fleischmann A, et al. Does quantification of USPIO uptake-related signal loss allow differentiation of benign and malignant normal-sized pelvic lymph nodes? Contrast Media Mol Imaging 2012;7:346-55.
26. Jung CW. Surface properties of superparamagnetic iron oxide MR contrast agents: ferumoxides, ferumoxtran, ferumoxsil. Magn Reson Imaging 1995;13:675-91.
27. Jung CW, Jacobs P. Physical and chemical properties of superparamagnetic iron oxide MR contrast agents: ferumoxides, ferumoxtran, ferumoxsil. Magn Reson Imaging 1995;13:661-74.
28. Bordat C, Sich M, Réty F, et al. Distribution of iron oxide nanoparticles in rat lymph nodes studied using electron energy loss spectroscopy (EELS) and electron spectroscopic imaging (ESI). J Magn Reson Imaging 2000;12:505-9.
29. Weissleder R, Elizondo G, Wittenberg J, et al. Ultrasmall superparamagnetic iron oxide: an intravenous contrast agent for assessing lymph nodes with MR imaging. Radiology 1990;175:494-8.
30. Varallyay CG, Nesbit E, Fu R, et al. High-resolution steady-state cerebral blood volume maps in patients with central nervous system neoplasms using ferumoxytol, a superparamagnetic iron oxide nanoparticle. J Cereb Blood Flow Metab 2013;33:780-6.
31. Sirlin CB, Reeder SB. Magnetic resonance imaging quantification of liver iron. Magn Reson Imaging Clin N Am 2010;18:359-81, ix.
32. Heesakkers RA, Fütterer JJ, Hövels AM, et al. Prostate cancer evaluated with ferumoxtran-10-enhanced T2*-weighted MR Imaging at 1.5 and 3.0 T: early experience. Radiology 2006;239:481-7.
33. Meijer HJ, Fortuin AS, van Lin EN, et al. Geographical distribution of lymph node metastases on MR lymphography in prostate cancer patients. Radiother Oncol. 2013 Jan;106(1):59-63. Epub 2012 Nov 27. Erratum in: Radiother Oncol 2013;107:442.
34. Fortuin AS, Smeenk RJ, Meijer HJ, et al. Lymphotropic nanoparticle-enhanced MRI in prostate cancer: value and therapeutic potential. Curr Urol Rep 2014;15:389.
35. Fortuin AS, Barentsz JO. Comments on Ultrasmall superparamagnetic particles of iron oxide allow for the detection of metastases in normal sized pelvic lymph nodes of patients with bladder and/or prostate cancer, Triantafyllou et al., European Journal of Cancer, published online 22 October 2012. Eur J Cancer 2013;49:1789-90.
36. Heesakkers RA, Jager GJ, Hövels AM, et al. Prostate cancer: detection of lymph node metastases outside the routine surgical area with ferumoxtran-10-enhanced MR imaging. Radiology 2009;251:408-14.
37. Meijer HJ, van Lin EN, Debats OA, et al. High occurrence of aberrant lymph node spread on magnetic

resonance lymphography in prostate cancer patients with a biochemical recurrence after radical prostatectomy. Int J Radiat Oncol Biol Phys 2012;82:1405-10.
38. Wu L, Cao Y, Liao C, et al. Diagnostic performance of USPIO-enhanced MRI for lymph-node metastases in different body regions: a meta-analysis. Eur J Radiol 2011;80:582-9.
39. Bernd H, De Kerviler E, Gaillard S, et al. Safety and tolerability of ultrasmall superparamagnetic iron oxide contrast agent: comprehensive analysis of a clinical development program. Invest Radiol 2009;44:336-42.
40. Bailie GR. Comparison of rates of reported adverse events associated with i.v. iron products in the United States. Am J Health Syst Pharm 2012;69:310-20.
41. Toth GB, Varallyay CG, Horvath A, et al. Current and potential imaging applications of ferumoxytol for magnetic resonance imaging. Kidney Int 2017;92:47-66.
42. Rampton D, Folkersen J, Fishbane S, et al. Hypersensitivity reactions to intravenous iron: guidance for risk minimization and management. Haematologica 2014;99:1671-6.
43. Pesapane F, Nazzaro G, Gianotti R, et al. A short history of tattoo. JAMA Dermatol 2014;150:145.
44. Sankineni S, Brown AM, Fascelli M, et al. Lymph node staging in prostate cancer. Curr Urol Rep 2015;16:30.
45. Harisinghani M, Ross RW, Guimaraes AR, et al. Utility of a new bolus-injectable nanoparticle for clinical cancer staging. Neoplasia 2007;9:1160-5.
46. Turkbey B, Agarwal HK, Shih J, et al. A Phase I Dosing Study of Ferumoxytol for MR Lymphography at 3 T in Patients With Prostate Cancer. AJR Am J Roentgenol 2015;205:64-9.
47. FDA Drug Safety Communication: FDA strengthens warnings and changes prescribing instructions to decrease the risk of serious allergic reactions with anemia drug Feraheme (ferumoxytol) 2015. Available online: https://www.fda.gov/drugs/drugsafety/ucm440138.htm
48. Auerbach M, Strauss W, Auerbach S, et al. Safety and efficacy of total dose infusion of 1,020 mg of ferumoxytol administered over 15 min. Am J Hematol 2013;88:944-7.

Cite this article as: Czarniecki M, Pesapane F, Wood BJ, Choyke PL, Turkbey B. Ultra-small superparamagnetic iron oxide contrast agents for lymph node staging of high-risk prostate cancer. Transl Androl Urol 2018;7(Suppl 4):S453-S461. doi: 10.21037/tau.2018.05.15

